applied sciences

MDPI

Article

Optimization and Economic Analysis for Small-Scale Movable LNG Liquefaction Process with Leakage Considerations

Sang Hyun Lee [1], Dong-Ha Lim [2] and Kyungtae Park [1,*]

[1] Department of Chemical and Biological Engineering, Sookmyung Women's University, Seoul 04310, Korea; kiwi652@sookmyung.ac.kr

[2] Green Materials & Process R&D Group, Korea Institute of Industrial Technology, 55 Jongga-ro, Jung-gu, Ulsan 44413, Korea; dongha4u@kitech.re.kr

* Correspondence: ktpark@sm.ac.kr; Tel.: +82-2-2077-7084

Received: 10 July 2020; Accepted: 3 August 2020; Published: 4 August 2020

Abstract: In this study, exergy and economic analysis were conducted to gain insight on small-scale movable LNG liquefaction considering leakage. Optimization and comparison were performed to demonstrate the quantitative results of single mixed refrigerant, dual nitrogen expansion, and the propane pre-cooling self-refrigeration processes. For the optimization, exergy efficiency was used as the objective function; the results showed that exergy efficiencies are 38.85%, 19.96%, and 13.65%, for single mixed refrigerant, dual nitrogen expansion, and propane pre-cooling self-refrigeration, respectively. Further, the cost analysis showed that the product cost of each process is 4002.3 USD/tpa, 5490.2 USD/tpa, and 9608.5 USD/tpa. A sensitivity analysis was conducted to determine parameters that affect exergy and cost. The SMR process is the most competitive in terms of exergy efficiency, product cost, and operability, without considering makeup facilities.

Keywords: small-scale movable liquefied natural gas plant; particle swarm optimization; economic analysis; exergy analysis; single mixed refrigerant liquefaction process; nitrogen expansion liquefaction process; propane pre-cooling self-refrigeration process

1. Introduction

Energy demand has gradually increased from the last decade because of the economic development and population growth around the world [1]. Liquefied natural gas (LNG) is becoming a primary energy resource in the global energy market owing to its cleanness, ease of transportability, and lower greenhouse gas emissions compared to other fossil fuels [2]. These positive advantages of LNG have attracted considerable attention in view of the current energy crisis.

Liquefying natural gas and pipeline transportation are two major methods for transporting natural gas. However, the pipeline method is not economical for long-distance transportation because of unstable gas flow rates [3]. Therefore, liquefying natural gas can be the best method to transport natural gas across the ocean.

The international gas union reported that various countries are constructing LNG liquefaction plants because of their rapidly growing reliance on natural gas from Asia to America [4]. Thus far, centralized large-capacity LNG liquefaction plants have been widely used; however, there has been an increasing interest toward distributed LNG liquefaction systems because of isolated small natural gas reservoirs [3], energy supply to isolated areas, and LNG bunkering systems [5]. Distributed LNG liquefaction plants can be classified into small-scale liquefaction plants with capacities of less than 40 million standard cubic feet per day or about 700 tonne per day (tpd) [6]. To satisfy the growing

demand of LNG, movable and economically efficient small-scale LNG processes such as single mixed refrigerant (SMR) process and expander cycle have been studied [7].

Energy and exergy efficiencies are key factors for evaluating the performance of small-scale LNG processes [8]. Khan and Lee employed particle swarm optimization (PSO) on the SMR process to enhance exergy efficiency, and the result of enhanced exergy efficiency was 50.77% after optimization [9]. Qyyum et al. [10] proposed a dual effect SMR (DSMR) LNG liquefaction cycle that has relatively lower cost and energy efficiencies. The DSMR process uses a SMR loop that separates into dual cooling and subcooling loops, and it can replace the classical dual mixed refrigerant process. Further, they reported that the exergy efficiency of the DSMR process is 36.62% and the total annualized cost is 1565 MM USD/year. Qyyum et al. [11] attempted to replace a Joule-Thomson (JT) valve with a hydraulic turbine (HT) in the SMR process to improve energy and exergy efficiencies. The energy consumption reduced up to 16.5% and the exergy efficiency can be improved up to 10.95% compared to the conventional SMR process. The effect of the number of mixed refrigerant (MR) components in the SMR process was investigated by Tianbiao et al.; they concluded that energy and exergy efficiencies increased with an increase in the number of MR components [12]. Qyyum et al. [13] proposed a hybrid modified coordinate descent (HMCD) algorithm to optimize the SMR process. They compared the optimization performance of the HMCD to other optimization algorithms such as PSO, knowledge-based optimization, and genetic algorithm. The HMCD showed better performance in terms of energy savings and coefficient of performance compared to other optimization algorithms.

Although the SMR process has higher energy and exergy efficiency compared to the nitrogen expansion cycle, the nitrogen expansion cycle is suited for small-scale LNG liquefaction because it is more safe and easy to operate [14]. The nitrogen expansion cycle has been studied by several researchers. He and Ju [15] proposed a novel conceptual design of parallel nitrogen expansion liquefaction for small-scale plants. They installed expanders in parallel to reduce the temperature difference, which can help achieve high exergy efficiencies. Thus, their proposed process could reduce the unit energy consumption by 4.69% compared to the conventional nitrogen expansion liquefaction. Further, He and Ju [16] investigated the performance of the two different refrigerants (R410a and propane) for pre-cooling the nitrogen expansion cycle. They optimized three different processes using specific energy consumption as the objective function and proved that nitrogen expansion with the R410a pre-cooling cycle is better than that with or without the propane pre-cooling cycle. Yuan et al. [17] proposed a novel small-scale liquefaction that uses single nitrogen expansion with a carbon dioxide pre-cooling cycle. They compared the energy consumption of the proposed process with three different small-scale LNG liquefaction cycles such as a propane pre-cooling MR cycle, an N_2-CH_4 expander cycle, and a modified mixed refrigerant cycle (MRC). They concluded that the proposed cycle achieved the lowest energy consumption (9.90 kWh/kmol) among all compared processes and insisted on the advantages of considerable stability and simple capability of their process. Qyyum et al. [18] proposed the closed-loop self-cooling recuperative N_2 expander cycle, wherein they added a recuperator to the single nitrogen expansion cycle to reduce exergy losses. In addition, after performing optimization configurations of the proposed process, they concluded that a configuration with a natural gas feed expander can save up to 22.2% of the required energy compared to the base case.

Self-refrigeration LNG liquefaction based on the Linde-Hampson cycle is another improvement in the natural gas liquid (NGL) recovery process [19]. The gas from the separator is partially vaporized, and this vapor is then used as the refrigerant in the cycle to cool the inlet gas. This process is called self-refrigeration, and it can reduce the refrigeration duty of the cooling cycle and the required amount of refrigerants [19]. Unfortunately, there have been few studies regarding the self-refrigeration process. The LNG production and transportation company Galileo Technologies developed a small-scale movable LNG liquefaction plant by applying the self-refrigeration technology to their product called Cryobox®; this is an actual commercialized movable LNG production plant [20].

Although various studies developed the LNG liquefaction process, only a few studies focus on the leakage problem on the compressors. Previous studies focused on developing new processes with high

exergy or energy efficiency, performing optimizations to increase efficiency, or varying the composition of the refrigerant. Ravukumar et al. [21] pointed out that the potential problem of LNG liquefaction plants is the refrigerant leak from the compressors. Further, the leakage problem can cause considerable problems for entire system, especially in small-scale LNG liquefaction systems where the compressors and seal systems are not leak-tight [22]. Consequently, the sustainability of the LNG liquefaction plants can be improved by solving this leakage problem. The refrigerant leakage problem can be resolved using a makeup system. Although it is easy for large-scale LNG plants to compensate for the leaked refrigerant using an NGL fractionation unit; this is not an economical option for small-scale LNG plants [23]. Therefore, small-scale LNG plants or movable LNG plants need to consider extra external makeup facilities for the leaked refrigerant or to use less leaking compressors [22].

In this study, three LNG liquefaction processes for a small-scale movable LNG liquefaction plant: SMR, dual nitrogen expansion, and propane pre-cooled self-refrigeration are investigated considering compressor leakage. To analyze the thermodynamics and economics, exergy efficiency, and product cost of all three processes are calculated in this study. The product cost of a small-scale movable LNG plant is not very economically favored compared to medium to large-scale businesses. However, small-scale movable LNG plant can be considered the first alternative for businesses that require a lower CAPEX and relatively simple on-site infrastructure [24]. Therefore, this paper analyzes whether it is reasonable to have a makeup system to resolve the leakage problem in terms of product cost. This paper is expected to provide more realistic insight into small-scale movable LNG liquefaction plants considering leakage problems to meet the growing demand for small-scale movable LNG plants.

The rest of this paper is organized as follows: The process descriptions of the three LNG liquefaction processes are proposed in Section 2. Further, in this section, the initial conditions of the simulation models and the optimization framework are introduced in detail. Exergy analysis and the cost analysis results are shown with the optimized model in Section 3. The effect of the refrigerant compositions, ambient temperature, electricity cost, and leakage rate on the thermodynamics and economics are investigated via a sensitivity analysis in Section 4. Finally, the conclusion of this study is provided in Section 5.

2. Methods

2.1. Process Description

Since most energy supply systems are operated under a centralized energy system concept [25], the movable LNG liquefaction plant is considered as an alternative for a distributed energy system. This plant can be used to supply LNG to an energy-supply isolated area or in transportation such as on trucks or ships. This study aims to investigate a movable LNG liquefaction plant that comprises compressors/expanders, JT-valves, separators, LNG storage drums, and a motor room as shown in Figure 1.

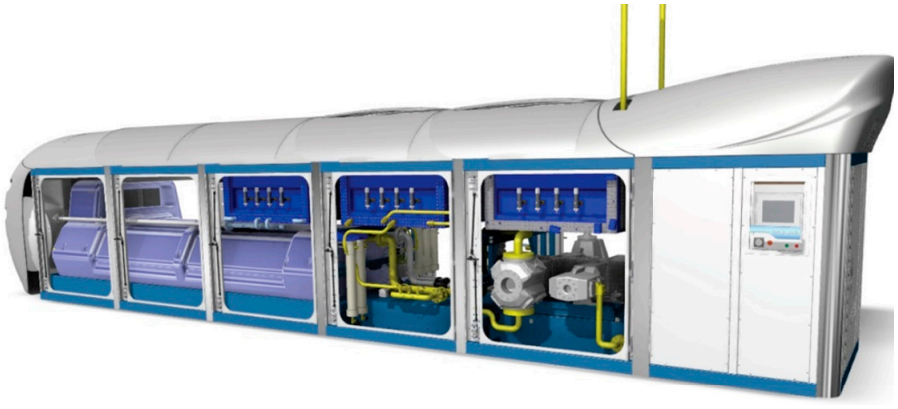

Figure 1. Illustration of a movable liquefied natural gas liquefaction plant.

The SMR, N_2 expansion, and propane pre-cooled self-refrigeration processes for the movable LNG liquefaction plant are considered in this study because they have been extensively studied for small-and medium-scale LNG plants owing to their low capital expenditures [26], low equipment count, and simple process configuration [27].

2.1.1. Single Mixed Refrigerant (SMR)

Figure 2 shows a schematic of the SMR process, which is the simplest natural gas liquefaction system. The SMR process comprises a MR compressor with an associated after-cooler, a main cryogenic heat exchanger (MCHE), JT valves, and a separator. In this process, the feed gas is liquefied in the MCHE, and the liquefied feed gas is then expanded by the JT-NG to separate non-condensable gases from the final product to meet the required LNG conditions. The required cold energy is provided by the MR, that consists of nitrogen, methane, ethane, propane, and butane.

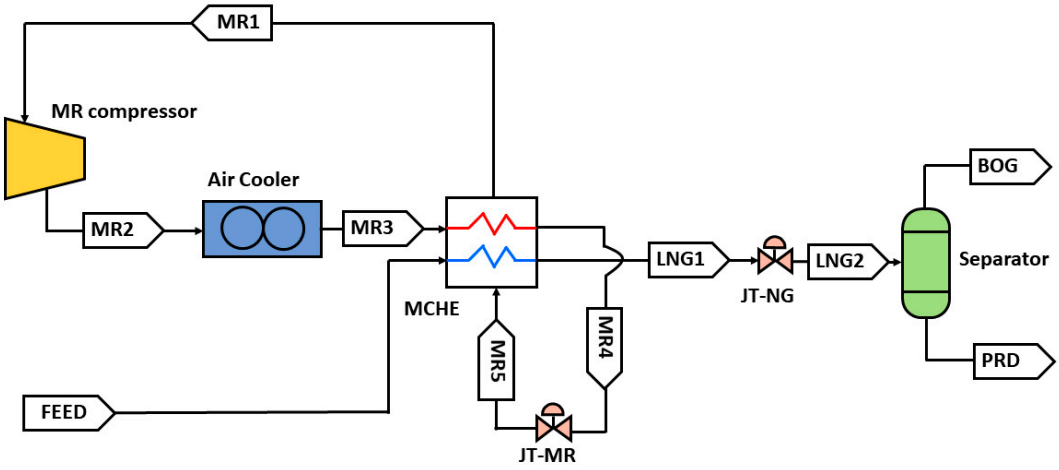

Figure 2. Process flow diagram of the single mixed refrigerant system.

2.1.2. Dual Nitrogen Expansion

Dual nitrogen expansion uses a reverse Brayton cycle to liquefy natural gas using nitrogen as a refrigerant [28]. The reverse Brayton cycle uses only the sensible heat of the refrigerant to transfer cold energy to natural gas so that the volume of the refrigerant is relatively larger than that of the SMR process. In this process, the external work is provided by an N_2 compressor, and then, a cold and warm expander transforms the pressure energy to cold energy [29]. Dual nitrogen expansion uses two expanders working at different range of temperature, endeavor to extract the maximum sensible heat from the refrigerant to liquefy natural gas [30]. A schematic of the dual nitrogen expansion cycle is shown in Figure 3.

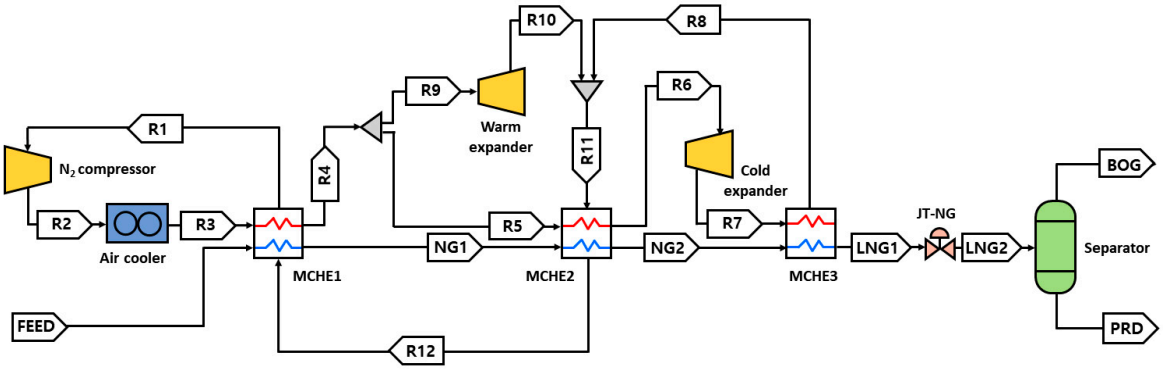

Figure 3. Process flow diagram of the dual nitrogen expansion system.

2.1.3. Propane Pre-Cooled Self-Refrigeration

Propane pre-cooled self-refrigeration is based on the Linde-Hampson liquefaction cycle and the overall process is shown in Figure 4. In the Linde-Hampson liquefaction cycle, the highly compressed gas is cooled down in heat exchangers using the returned low-pressure stream, and it is then moved to the JT valve to expand [29]. This process is the enhanced Linde-Hampson liquefaction cycle that adopts a propane precooling loop to achieve better performance [30]. This liquefaction process requires higher pressure (>200 bar) than other liquefaction processes to produce cold energy by expansion. Thus, a low process efficiency is inevitable.

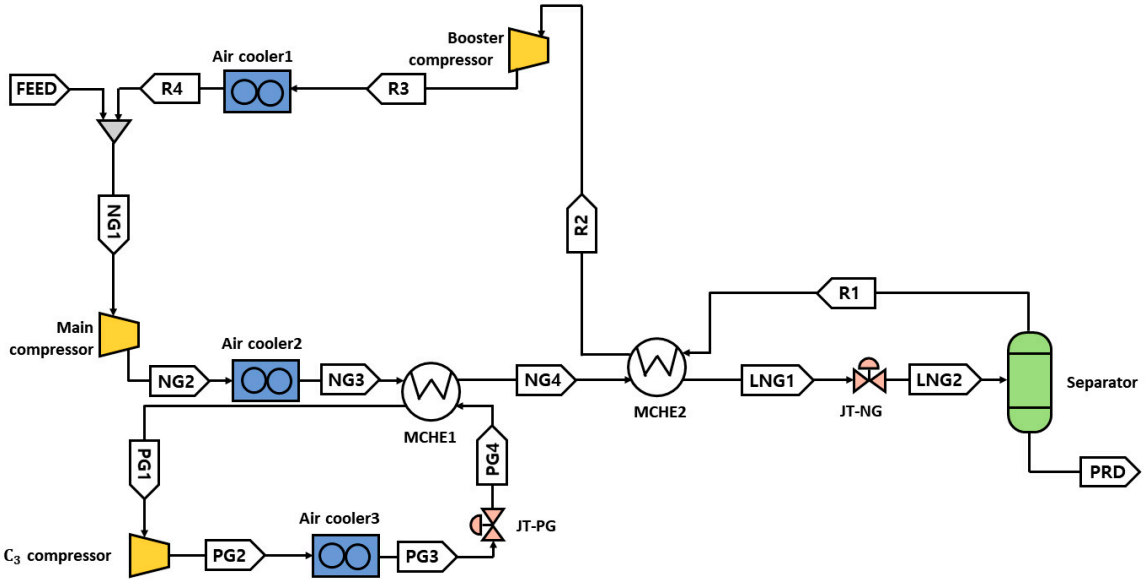

Figure 4. Process flow diagram of the propane pre-cooled self-refrigeration system.

2.1.4. Compressor Leak Consideration

The potential problem of a movable LNG liquefaction plant is a refrigerant leak from the compressor. Compressor leaks without refrigerant make-up causes severe operational problems such as poor efficiency and variations in operating conditions [31]. All compressors in the liquefaction processes compared in this study are assumed to be reciprocating compressors because of their small capacity.

The main cause of leaks in reciprocating compressors is valve leakages. Therefore, according to [32], newly installed packing has been reported to leak an average of 2 m^3/h and worn packing may leak up to an average of 26 m^3/h. Further, the leakage rates vary with production size; thus, the average leakage rate for a small-size production compressor is 0.31–0.34 m^3/h, and it is the large compressors may leak 0.68–4.25 m^3/h for large compressors [33]. Ferreira [34] reported that the leakage through the clearance of the compressor depends on the actual radial clearance and thus, the total leak mass varies in the range of 0.017–0.443 kg/h with 2.75–12 μm of radial clearance. Based on previous studies and our project experience, the leakage rate of reciprocating compressors is fixed to 0.05 wt. % of the total amount of refrigerant in this study. The compressor leak can be also solved using compressors with high leakage resistance such as a Labyrinth sealed compressor; however, this solution is not considered in this paper [22].

As the target LNG liquefaction plant is movable, an additional leakage makeup system for each process is required to make up the refrigerants. The schematics for each refrigerant make up system are shown Figure A1(3). The SMR system is supposed to have separate tanks for all component of the refrigerants and a mixing tank for mixing the refrigerants [35]. In the case of dual nitrogen expansion, liquid nitrogen is supplied for the leakage make up [36]; for propane pre-cooled self-refrigeration, only propane makeup facilities are required.

2.1.5. Initial Process Condition

To investigate the processes, all LNG liquefaction processes are simulated using a commercial simulator ASPEN PLUS V11 and the thermodynamic property Peng-Robinson (PR) equation of state is applied since PR is a widely used in the LNG processes [37–39]. All common parameters for each simulation case are summarized in Table 1. The process is based on actual project experience that produces 626 kg/h (15 tons per day) of LNG.

Table 1. Common parameters for all simulation cases.

Parameters [40,41]	Unit	Value
Feed NG compositions		Table 2
Feed NG flowrate	kg/h	626.4
Feed NG temperature	°C	20
Feed NG inlet pressure	bar	60
LNG production pressure	bar	1.05
LNG production temperature	°C	Saturated
Ambient temperature	°C	20
Pressure drop in heat exchangers	bar	0.2
Compressor adiabatic efficiency		0.8
Expander adiabatic efficiency		0.8

Table 2. Different feed natural gas compositions [40].

Component	Mole Fraction		
	Lean	Normal [(1)]	Rich
Nitrogen	0.0037	0.00185	0.000
Methane	0.9589	0.92345	0.888
Ethane	0.0296	0.0428	0.056
Propane	0.0072	0.0221	0.037
n-Butane	0.0003	0.0049	0.0095
i-Butane	0.0003	0.0049	0.0095

[(1)] The normal composition is the average value of lean and rich feed streams.

This study used three different natural gas compositions: lean, normal, and rich. The lean stream is chosen for the base case, and the others are adopted in the sensitivity analysis to investigate the effect of the natural gas compositions on the proposed processes.

2.2. Optimization Framework

Optimization was performed using the concept of exergy to determine the best operating conditions of the liquefaction processes.

Exergy analysis has been widely studied to evaluate the performance of a liquefaction system [8,42–44]. Exergy is defined as the maximum amount of useful energy that can be extracted from a reversible process [8]. Exergy can be calculated as [45]

$$Ex = (h_x - h_0) - T_0(s_x - s_0) \quad (1)$$

where h is the enthalpy of the stream, s is the entropy of the stream, and T is the temperature of the stream; subscript "0" indicates the reference state (at ambient temperature, 20 °C in this study) of enthalpy and entropy.

Exergy efficiency is an important factor for performing exergy analysis, and it is calculated as [14].

$$\eta_{ex} = \frac{\Delta Ex}{W_{net}} \tag{2}$$

where η_{ex} is the exergy efficiency, ΔEx is the total exergy supplied to the system, and W_{net} is the net power consumed. The total exergy supplied to the system can be formulated as

$$\Delta Ex = \sum Ex_{feed} - \sum Ex_{Product} \tag{3}$$

where Ex_{feed} is the exergy of feed streams, and $Ex_{product}$ is the exergy of the product streams. The total net power produced by the system can be formulated as

$$W_{net} = \sum W_{expander} - \sum W_{compressor} - \sum W_{pump} \tag{4}$$

where $W_{expander}$ is the energy produced by expanders, $W_{compressor}$ is the energy consumed by compressors, and W_{pump} is the energy consumed by pumps.

Finally, the objective function can be defined as

$$\text{Maximize. } f(x) = \text{Minimize}(-\eta_{ex}) \tag{5}$$

subject to

$$10 \le P_{MR2}^{SMR} \le 80 \tag{6}$$

$$-160 \le T_{LNG1,\,MR4}^{SMR} \le -150 \tag{7}$$

$$1.25 \le P_{LNG2}^{SMR} \le 10 \tag{8}$$

$$100 \le m_{MR,\ nitrogen}^{SMR} \le 800 \tag{9}$$

$$100 \le m_{MR,\,methane}^{SMR} \le 800 \tag{10}$$

$$500 \le m_{MR,\,ethane}^{SMR} \le 2000 \tag{11}$$

$$0 \le m_{MR,\,propane}^{SMR} \le 100 \tag{12}$$

$$500 \le m_{MR,\,butane}^{SMR} \le 2000, \tag{13}$$

$$10 \le P_{R1}^{DUAL} \le 20 \tag{14}$$

$$3000 \le m_{R1}^{DUAL} \le 10000 \tag{15}$$

$$40 \le P_{R2}^{DUAL} \le 80 \tag{16}$$

$$-20 \le T_{FEED}^{DUAL} \le 20 \tag{17}$$

$$-30 \le T_{R3}^{DUAL} \le 0 \tag{18}$$

$$-120 \le T_{NG1}^{DUAL} \le -80 \tag{19}$$

$$-160 \le T_{NG2}^{DUAL} \le -150 \tag{20}$$

$$0.5 \le x_{R9}^{DUAL} \le 0.8 \tag{21}$$

$$200 \le P_{NG2}^{SELF} \le 400 \tag{22}$$

$$5 \le P_{PG2}^{SELF} \le 20 \quad (23)$$

$$-40 \le T_{NG4}^{SELF} \le -20 \quad (24)$$

$$-100 \le T_{LNG1}^{SELF} \le -70 \quad (25)$$

$$1.25 \le P_{PG4}^{SELF} \le 5 \quad (26)$$

$$900 \le m_{PG1}^{SELF} \le 1300 \quad (27)$$

$$vf_{inlet,\ compressors} = 1 \quad (28)$$

$$vf_{inlet/outlet,\ expanders} = 1 \quad (29)$$

$$\text{MITA of the MCHE} \ge 2\text{K}, \quad (30)$$

where x is a set of the decision variables of the objective function, $x \in \{x_{SMR}, x_{DUAL}, x_{SELF}\}$. Equations (6)–(27) are boundary limits for decision variables; Equations (6)–(13) are for SMR ($x_{SMR} \in \{P_{MR2}^{SMR}, T_{LNG1,\ MR4}^{SMR}, P_{LNG2}^{SMR}, m_{MR,\ nitrogen}^{SMR}, m_{MR,\ methane}^{SMR}, m_{MR,\ propane}^{SMR}, m_{MR,\ butane}^{SMR}\}$), Equations (14)–(21) are for dual nitrogen expansion ($x_{DUAL} \in \{P_{R2}^{DUAL}, m_{R1}^{DUAL}, P_{R2}^{DUAL}, T_{FEED}^{DUAL}, T_{R3}^{DUAL}, T_{NG1}^{DUAL}, T_{NG2}^{DUAL}, x_{R9}^{DUAL}\}$), and Equations (22)–(27) are for propane-precooling self-refrigeration process ($x_{SELF} \in \{P_{NG2}^{SELF}, P_{NG2}^{SELF}, T_{NG4}^{SELF}, T_{LNG1}^{SELF}, P_{PG4}^{SELF}, m_{PG1}^{SELF}\}$). Equations (28)–(30) are the constraints set up for practical optimization results. Equations (28) and (29) are for protecting the compressors and expanders from the damage caused by liquid droplets, and Equation (30) [44] is for avoiding irreversibility and achieving better exergy efficiency. Therefore, the number of decision variables for SMR is 7, 8 for dual nitrogen expansion, and 6 for propane-precooling self-refrigeration. In addition, the number of constraints for SMR is 2, 6 for dual nitrogen expansion, and 5 for propane-precooling self-refrigeration.

In the sensitivity analysis, additional constraints are added to consider liquefaction as an as-built plant, which means the duty of the motor-driven equipment and heat transfer area of the heat exchangers are fixed. The additional constraints are

$$\text{MCH E's UAs} = \text{UA values from the optimized base case} \quad (31)$$

$$\begin{aligned} &\text{Compressors and expanders duties} \\ &\le \text{Compressors and expanders duties from the optimized base case} \end{aligned} \quad (32)$$

Since the UA values of the MCHE (overall heat transfer coefficient, U, multiplied by the heat transfer area, (A) are fixed, Equation (31) is deactivated in the sensitivity analysis. The specific constraint values for Equations (31) and (32) are summarized in Appendix A.2.

In this paper, optimization was performed using the PSO algorithm because of the high nonlinearity of the optimization problem formulated in this study [15,17–19]. The flowchart of the PSO algorithm is provided in Figure A2 and the detailed parameters used in this study are summarized in Table 3.

Table 3. Particle swarm optimization algorithm parameters used in this study.

Parameters	Value
Number of particles	10 × the number of decision variables
Maximum iteration	200
Self-adjustment weight	1.49
Social-adjustment weight	1.49
Stop criteria	1.0×10^{-6}

2.3. Economic Analysis Framework

The economic analysis is conducted to evaluate the different processes because it provides a comprehensive understanding of the process [46]. The cost estimation framework used in this study is illustrated in Figure 5. The assumptions considered for the economic analysis are summarized in Table 4 [47–49].

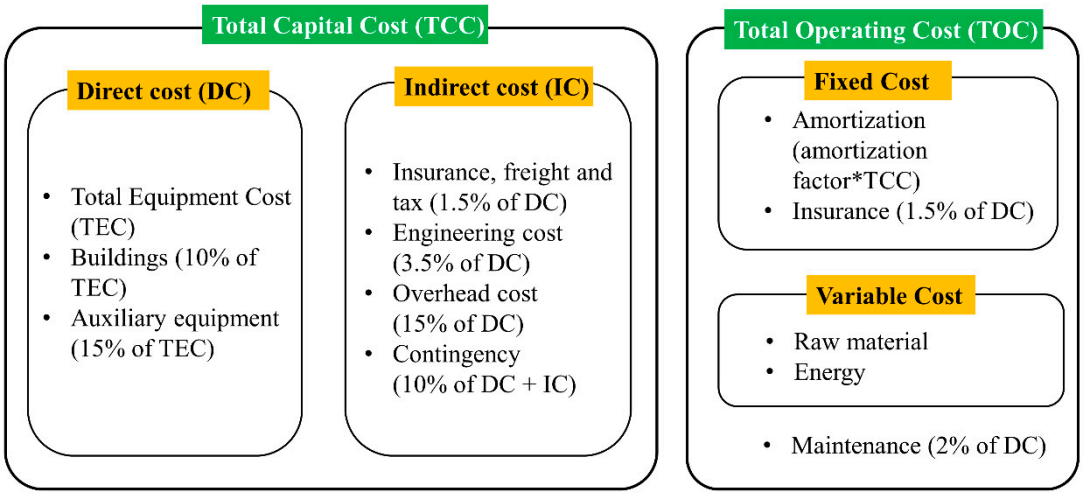

Figure 5. Cost estimation framework.

Table 4. Assumptions for economic analysis.

Assumptions
• All costs are presented in USD (2017).
• Plant availability of 95% corresponds to an operation time of 8322 h/year [49].
• Total equipment cost (TEC) is evaluated using Aspen process economic analyzer (2017) [49,50].
• As the land and labor costs vary depending on the scenario; they are not considered in this study.
• Total raw material costs include the initial charge and make-up costs of the material: the compressor leakage rate of 0.05 wt. % is assumed [32–34].
• Electricity costs are based on the average retail electricity prices in the US ($0.1048 per kWh) in 2017 [51].

The amortization factor (α) represents the annual repayment of the total capital cost (TCC); it is computed as

$$\alpha = \frac{i(1+i)^n}{(1+i)^n - 1} \tag{33}$$

where i represents the interest rate (8%) and n represents the plant lifetime (25 years) [51].

To calculate the raw material cost, this study considered both the initial charge cost and the leakage makeup cost as mentioned earlier. The total raw material cost of variable cost can be calculated

$$\text{Raw material cost} = \left(\frac{\text{initial charge cost}}{n} + \text{leakage makeup cost}\right) \times \frac{\text{CEPCI (2020)}}{\text{CEPCI (2017)}} \tag{34}$$

The raw material cost is adjusted based on the chemical engineering plant cost index (CEPCI) because some material costs are based on 2007 and 2020 prices [52]. The CEPCI for 2020 is 599.5; 2017 is 567.5; and 2007, 525.4 [53].

The considered raw materials in this study are: methane and natural gas, $0.21/kg [54]; ethane, $0.534kg [55]; propane, $0.679/kg [56]; butane, $0.702/kg [57]; and nitrogen $0.546/kg [58]. As methane

has the largest proportion in the composition of the natural gas, the price of the methane is assumed to be the price of the natural gas.

The total annualized cost (TAC) is calculated as

$$\mathrm{TAC} = \frac{\mathrm{TCC}}{n} + \mathrm{TOC} \tag{35}$$

Product cost is a useful index to compare *LNG* liquefaction plants regardless of its capacity [24]; the product cost is calculated as

$$Product\ cost\left(\frac{USD}{tpa}\right) = \frac{TCC + TOC * n * plant\ availability}{LNG\ production\ rate} \tag{36}$$

where n represents the plant lifetime and the plant availability is 95%.

3. Results

Base Case

To verify the performance of the PSO algorithm, the performance of three different optimization algorithms are compared and results are shown in Figure 6. The performance comparison between the pattern search (PS), the genetic algorithm (GA), and the PSO algorithm was investigated for the base case. Also, the execution time of each algorithm for the base case is summarized in Table 5. As shown in Figure 6 and Table 5, the PSO algorithm shows the best performance work and the shorted execution time compared to the other two algorithms. Consequently, this paper conducted the rest of the optimization by utilizing the PSO algorithm.

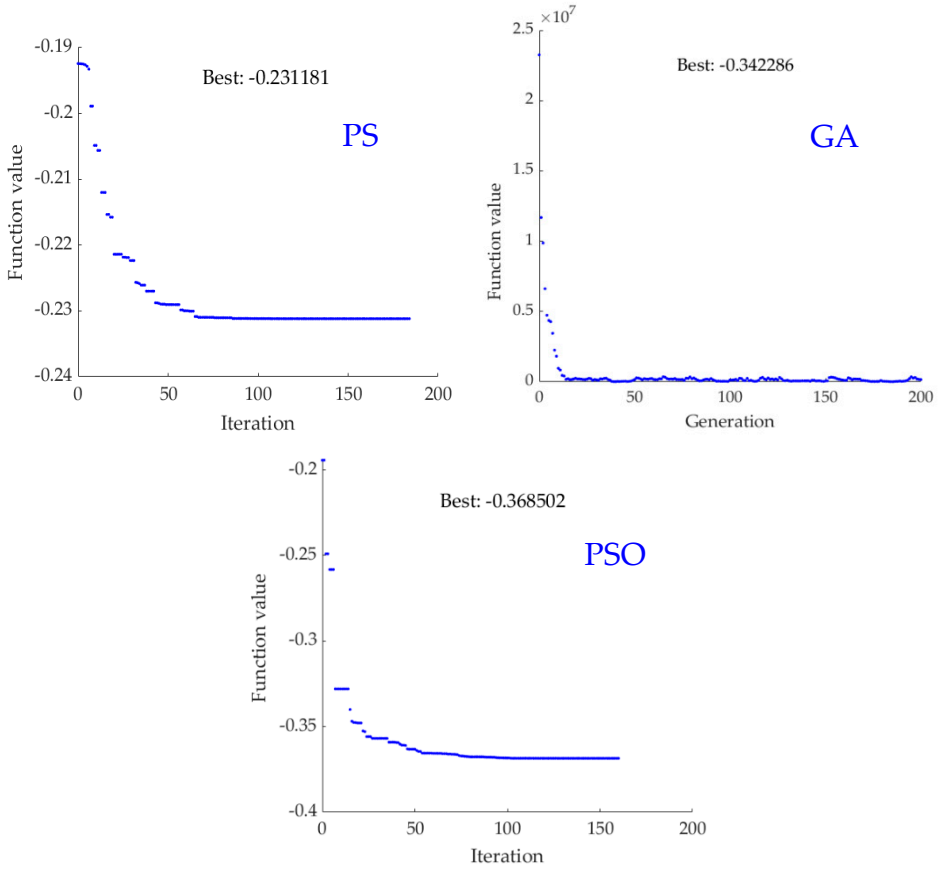

Figure 6. Performance comparison results of optimization algorithms for the base case.

Table 5. Execution time comparison of optimization algorithms for the base case.

Optimization Algorithm	Execution Time (Min.)
Patter search	241.8
Genetic algorithm	533.2
Particle swarm optimization	132.2

The base case adopts the lean natural gas and the optimized results of each process are summarized in Table A4(6); Figure 7 shows exergy efficiency and TAC of each case. As shown in Figure 6, SMR has the highest exergy efficiency (38.85%) and the lowest TAC (0.888 MM USD/year). In contrast, propane pre-cooled self-refrigeration has the lowest exergy efficiency (13.65%) and the highest TAC (2.179 MM USD/year).

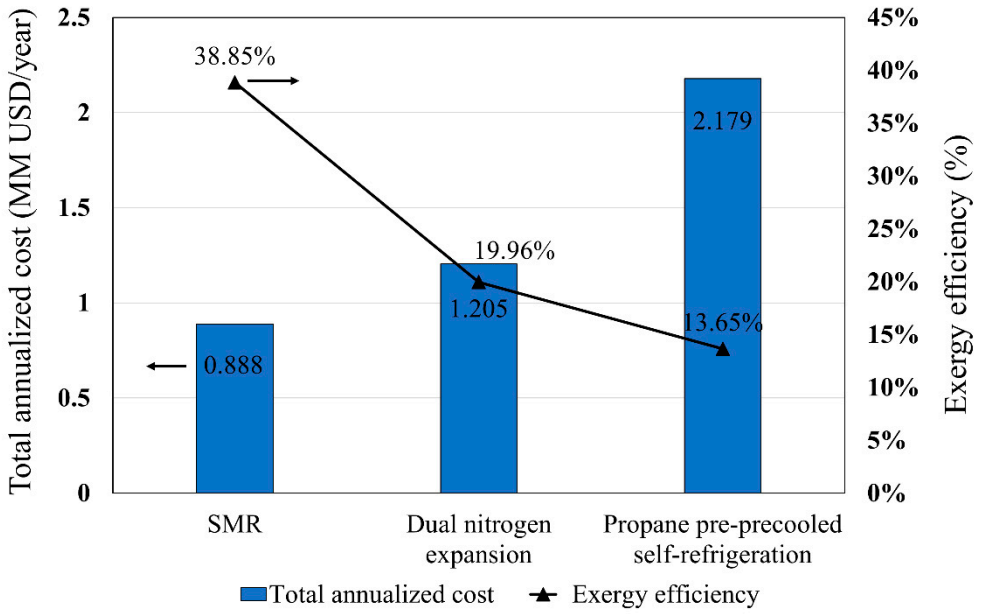

Figure 7. Exergy efficiency and the total annualized cost for each process.

The details of TAC are summarized in Table 6 and Figure 8 shows total equipment cost (TEC) breakdown of each process. As shown in Table 6, TAC of SMR (0.888 MM USD/year) is considerably lower than that of the others because of the low direct cost contributed by the simple process layout. According to Figure 8, the compressor costs comprises a significant portion of the TEC regardless of the process, and therefore, W_{net} and the number of compressors is the most important factors in the cost analysis. Further, W_{net} affects the variable cost because the energy cost comprises a large portion of the variable cost. The proportion of the makeup system in TEC of SMR is about 38.98%, which is remarkably higher than that of other processes because of mixed refrigerant. In contrast, the proportion of the makeup system in propane pre-cooled self-refrigeration does not seem to be significant (3.39%) because of the single (propane) refrigerant.

The product cost for propane pre-cooled self-refrigeration (10,213.5 USD/tpa) has the highest value, followed by that for dual nitrogen expansion (5645.4 USD/tpa) and SMR (4162.5 USD/tpa). According to the Oxford institute for energy studies [59], a capital expenditure (CAPEX) of small-scale movable LNG liquefaction usually ranges between 200–1600 USD/tpa. The CAPEX can be calculated by dividing TCC by the annual LNG production rate. The CAPEX for SMR, dual nitrogen expansion, and propane pre-cooled self-refrigeration investigated in this paper are 858.5 USD/tpa, 1069.9 USD/tpa, and 2064.9 USD/tpa, respectively. Therefore, the results of the CAPEX for the three processes are approximately in the range of 200–1600 USD/tpa, the economic analysis in this study appears reliable.

Table 6. Summary of the cost analysis results.

	SMR	Dual Nitrogen Expansion	Propane Pre-Cooled Self-Refrigeration
Total capital cost (TCC, MM USD)	4.394	5.477	10.568
Direct cost	3.329	4.149	8.006
Indirect cost	0.666	0.830	1.601
Contingency	0.399	0.498	0.961
Total operating cost (TOC, MM USD/yr)	0.712	0.986	1.756
Variable cost	0.182	0.326	0.483
Raw material cost	0.014	0.021	0.004
Energy cost	0.168	0.305	0.479
Fixed cost	0.463	0.577	1.113
Maintenance	0.067	0.083	0.160
Total annualized cost (TAC, MM USD/yr)	0.888	1.205	2.179
Product cost (USD/tpa)	4162.5	5645.4	10213.5

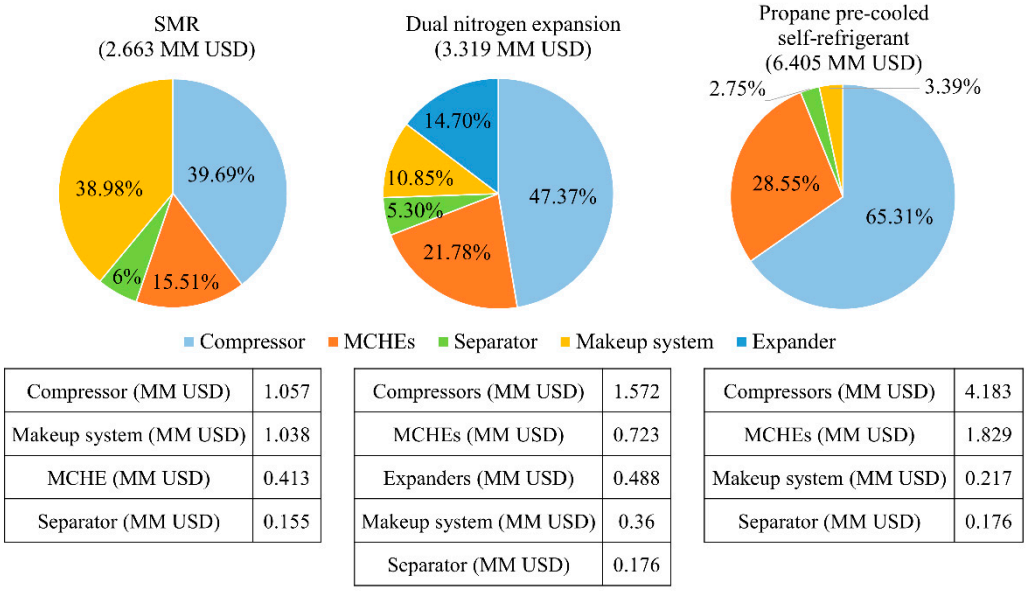

Compressor (MM USD)	1.057
Makeup system (MM USD)	1.038
MCHE (MM USD)	0.413
Separator (MM USD)	0.155

Compressors (MM USD)	1.572
MCHEs (MM USD)	0.723
Expanders (MM USD)	0.488
Makeup system (MM USD)	0.36
Separator (MM USD)	0.176

Compressors (MM USD)	4.183
MCHEs (MM USD)	1.829
Makeup system (MM USD)	0.217
Separator (MM USD)	0.176

Figure 8. Breakdown of the total equipment cost.

Figure 9 shows the compassion of TAC differences between the case with and without the refrigerant leakage consideration. As shown in Figure 8, TOC and TCC differences between both cases in SMR are significant because of the complex refrigerant make-up system. In contrast, TOC and TCC differences between both cases in other processes are not significant because of the simple make-up system.

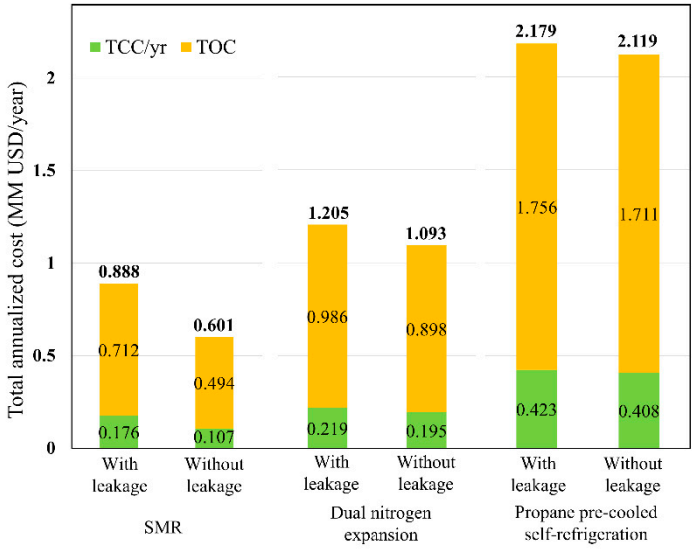

Figure 9. TAC comparison of the base case with/without the makeup system.

4. Sensitivity Analysis

4.1. Effect of Natural Gas Compositions

The analysis of the effect of natural gas composition on exergy efficiency is important because the target LNG plant in this study is movable, and because the uncertain effect of natural gas composition on exergy has already been reported [60]. As illustrated in Figure 10, the process most sensitive to natural gas compositions is SMR, which varies in the range of 36.85–37.46% (0.61%); propane pre-cooled self-refrigeration is the least sensitive and it varies in the range of 13.65–14.07% (0.42%). Overall, the effect of natural gas composition changes on exergy efficiency do not seem to be significant.

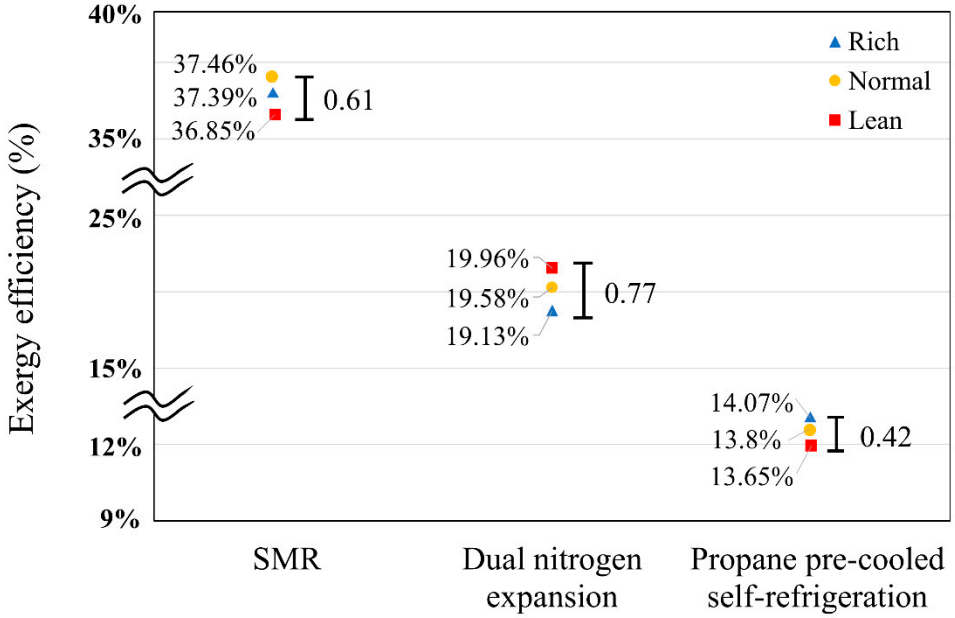

Figure 10. Effect of natural gas compositions on each process.

Figure 11 shows the effects of natural gas compositions on the product cost of each process. As shown in Figure 11, the product cost of all three processes tends to decrease as the composition becomes richer. However, the differences are not significant (about 3%) for all three processes.

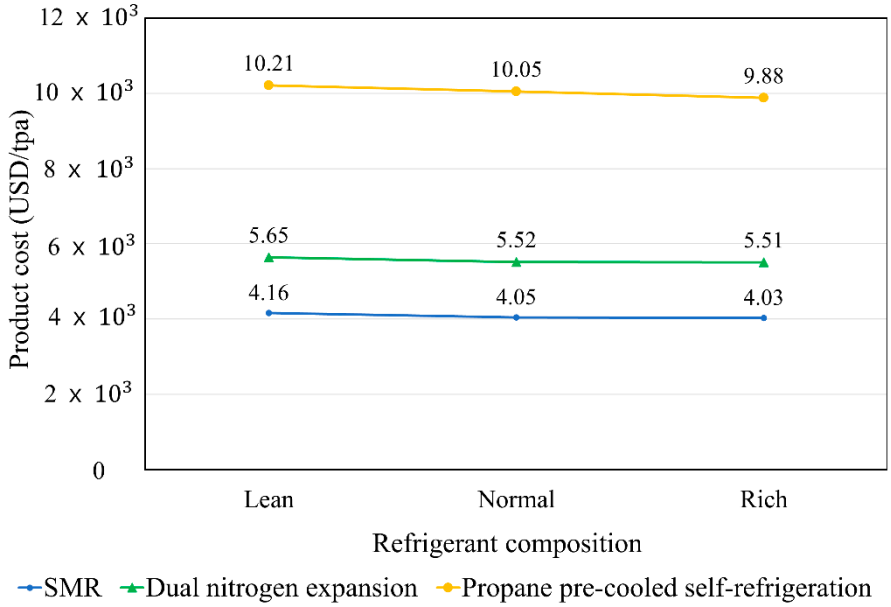

Figure 11. Effect of the natural gas compositions on the product cost of each process.

Figure 12 shows the effects of different natural gas composition on the variable cost. Even if leakage is considered, the raw material cost of all three processes is not affected by the composition of the natural gas. However, the energy cost of all three processes seems to be highly, and it tends to decrease from lean to rich. The largest differences in the variables cost can be seen for SMR (15.5%), followed by propane pre-cooled self-refrigeration (15%) and dual nitrogen expansion (9.18%).

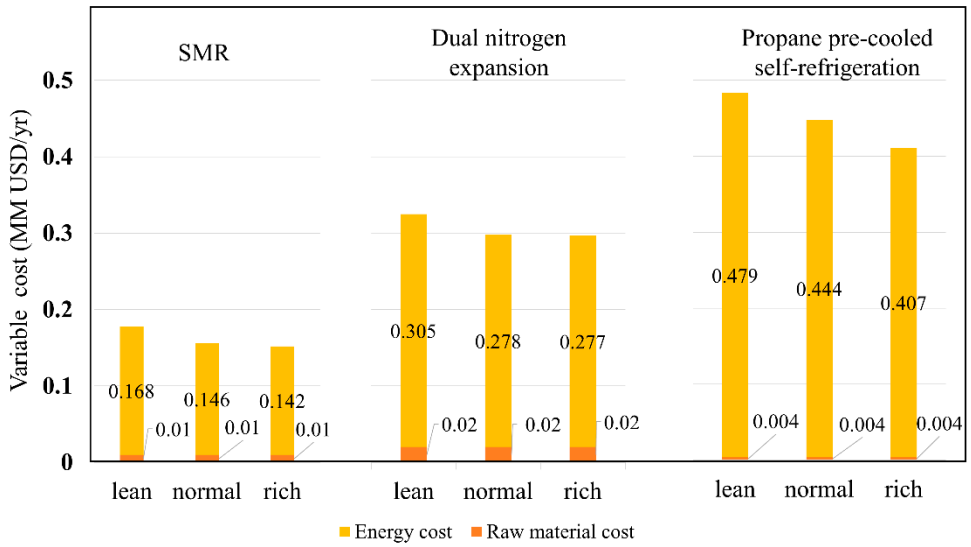

Figure 12. Effects of the natural gas compositions on the variable cost of each process.

4.2. Effect of Ambient Temperature

The temperature of the air cooler outlet stream varies according to ambient temperature. Therefore, the sensitivity analysis conducted to investigate the effect of ambient temperature on the exergy efficiency of each process and the results are illustrated in Figure 13. The air cooler discharge temperature is defined to be 10 °C higher than the ambient temperature. With an increasing ambient temperature value in the range of 0–40 °C with 5 °C step sizes, the exergy efficiency decreases in all three processes. The increase in the ambient temperature leads to an increment of the duties of the compressor and

the rise in the inlet temperatures of the MCHEs. Therefore, the required energy for liquefying the same natural gas capacity increases accordingly. The largest differences in the exergy efficiency can be observed in SMR (34.4%), followed by dual nitrogen expansion (22.3%) and propane pre-cooled self-refrigeration (5.08%). Each process has a certain temperature ranges that make the process infeasible because of the compressor duty constraint. The SMR process can operate over the wide range (10–40 °C) because it can adjust the MR composition according to the ambient temperature changes. However, the operation availability range of propane pre-cooled self-refrigeration is relatively small because of the refrigeration duty of the main compressor.

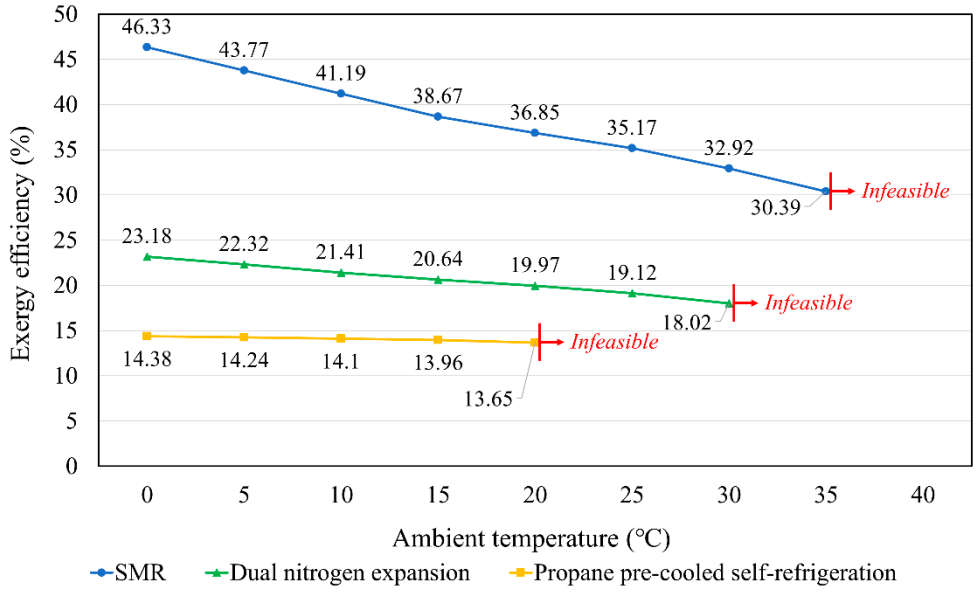

Figure 13. Effects of ambient temperature on exergy efficiency of each process.

The effects of ambient temperature on the product cost are illustrated in Figure 14. As stated earlier, an increase in the required energy affects the energy cost that leads to an increase in product cost. The largest difference in product cost can be observed for SMR, 5.9%; this is followed by dual nitrogen expansion (4.5%) and propane pre-cooled self-refrigeration (1.1%). Overall, the effect of the ambient temperature on the product cost does not seem to be significant.

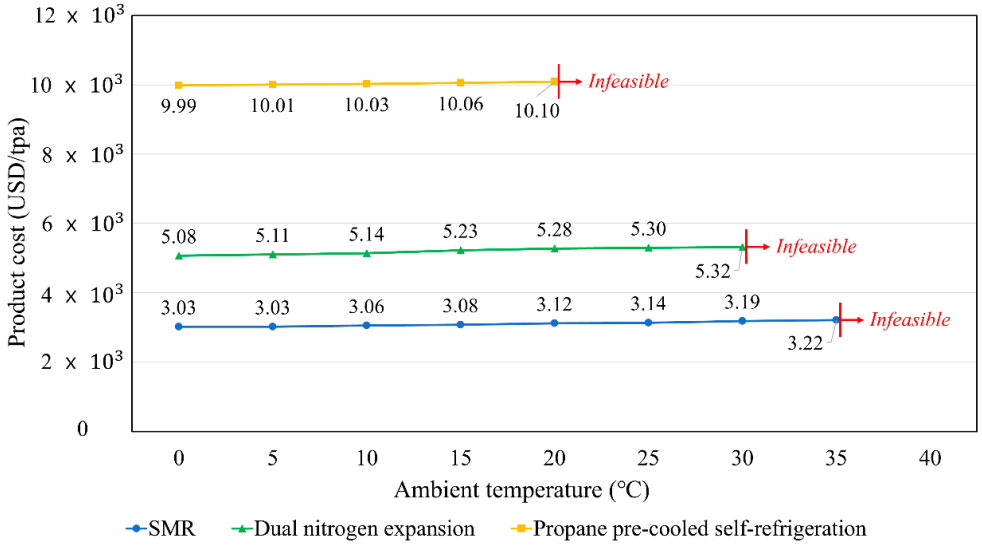

Figure 14. Effects of ambient temperature on product cost of each process.

4.3. Effect of Electricity Cost

Sensitivity analysis for the electricity cost is conducted because the energy cost occupies a large percentage of the total cost (Table 6), and the electricity cost varies widely within a given range. Figure 14 shows the effect of changes in the electricity cost on the product cost. The electricity cost varies between 0.08 and 2 $/kWh, and this range is referred from the previous studies [45,61]. As shown in Figure 15, the effect of the electricity cost on the product cost is to be significant. The SMR is the most affected with a 24.1% difference, followed by dual nitrogen expansion (23.9%) and propane pre-cooled self-refrigeration (21.7%).

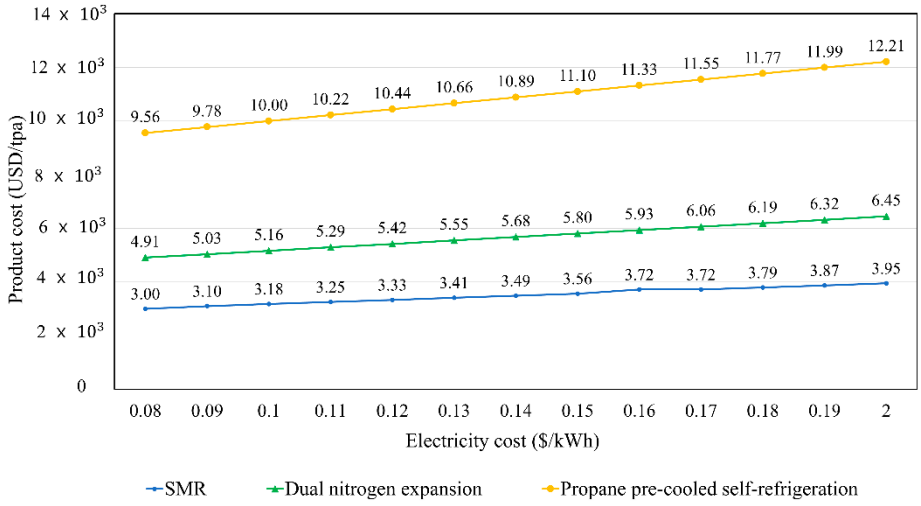

Figure 15. Effects of electricity cost on product cost of each process.

4.4. Effect of Compressor Leakage

Compressor leakage of the base case of the fixed to 0.05% to refrigerant mass flow rate, and it can differ within a range under certain conditions such as worn packing, product capacity, and actual radial clearance. To analyze the effect of different compressor leakage on the product cost, nine different weight percentages of leakage (0.01–1 wt. %) were selected to perform the sensitivity analysis.

Figure 15 shows the results of the product cost differences with respect to the compressor leakage. According to Figure 16, the effect of the compressor leakage on the product cost is not significant in propane pre-cooled self-refrigeration compared to other two processes. The largest differences in product cost among three processes was observed for SMR (3%), followed by dual nitrogen expansion (2.6%) and propane pre-cooled self-refrigeration (0.2%). This is because SMR requires an MR that consists of multiple hydrocarbon components to form the refrigerant, whereas dual nitrogen expansion only requires pure nitrogen as the refrigerant. Further, propane pre-cooled self-refrigeration requires a small amount of pure propane for the refrigerant leakage makeup.

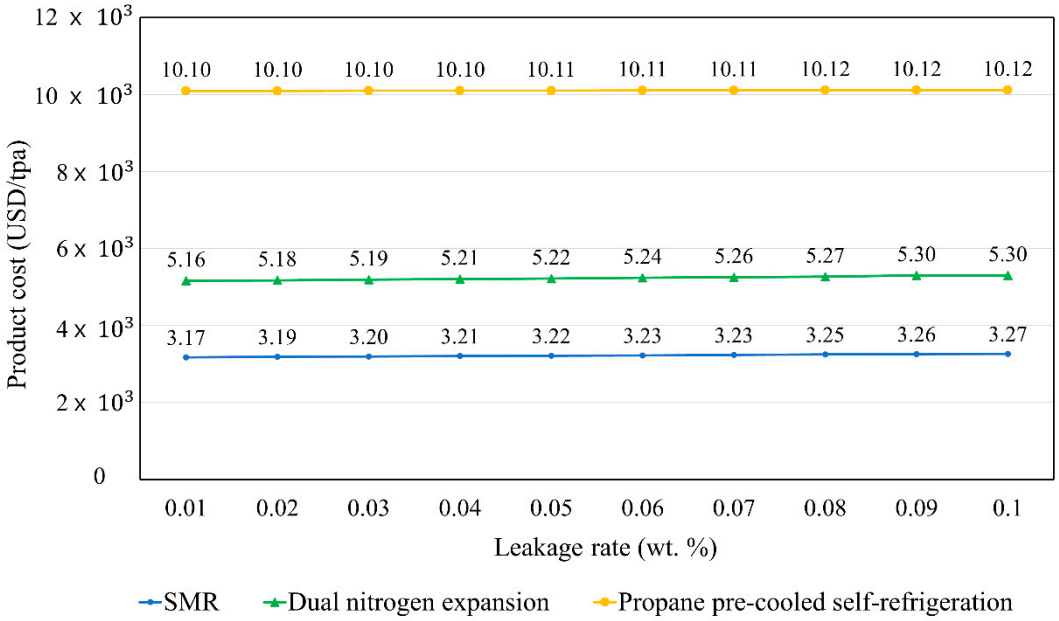

Figure 16. Effects of the compressor leakage on product cost of each process.

5. Conclusions

In this study, SMR, dual nitrogen expansion, propane pre-cooled self-refrigeration are investigated for a small-scale movable plant considering the compressor leakage. This paper presents a quantitative investigation of the three processes from the perspectives of exergy efficiency and cost analysis considering leakage problems.

The following conclusions were drawn based on the results of this study.

1. Optimization results indicated that SMR is the most efficient in terms of the exergy efficiency and economics even considering the makeup system. The addition of an extra makeup system significantly affects TAC of SMR compared to those of the others because SMR requires complex makeup facilities because of the MR. Yet, SMR is considered a competitive LNG liquefaction process for movable LNG plants.
2. Sensitivity analysis was performed to identify parameters that affect exergy and cost significantly. The results showed that natural gas composition, ambient temperature, and compressor leakage rate does not significantly affect product cost. However, effect of electricity cost on the product cost was found to be significant for all processes.
3. The effect of ambient temperature is noticeable from the perspective of exergy efficiency because the required energy tends to increase with an increase in ambient temperature. The SMR can operate within a wider range of ambient temperature changes compared to other processes.

This paper revealed that adding an extra external makeup system for small-scale movable LNG liquefaction not only solves the compressor leakage problem but also does not require significant financial expenditure compared to conventional small-scale movable LNG plants. Further, SMR is concluded to be the most suitable process for small-scale movable LNG plants because it exhibits the highest exergy efficiency, the lowest product cost considering makeup facilities, and the widest operation range. In future work, the safety and environmental issues of the refrigerant will be further investigated as these were excluded in this study.

Author Contributions: Conceptualization, K.P. and D.-H.L.; methodology, S.H.L.; writing—original draft preparation, S.H.L. and K.P.; data curation, S.H.L.; supervision, K.P.; funding acquisition, K.P.; All authors have read and agreed to the published version of the manuscript.

Funding: This research was funded by Sookmyung Women's University Research, grant number 1-1903-2001 and the National research foundation of Korea, grant number NRF-2018R1C1B5086306.

Conflicts of Interest: The authors declare no conflict of interest.

Nomenclature

Abbreviation	Description (Unit)
CAPEX	Capital expenditure (USD/tpa)
CEPCI	Chemical engineering plant cost index
COP	Coefficient of performance
DC	Direct cost (MM USD)
DSMR	Dual single mixed refrigerant
Gbest	Global best
GA	Genetic algorithm
HMCD	Hybrid modified coordinate descent
HT	Hydraulic turbine
IC	Indirect cost (MM USD)
IGU	International gas union
JT	Joule-Thomson
LNG	Liquefied natural gas
MCHE	Main cryogenic heat exchanger
MITA	Minimum internal temperature approach (K)
MM US	Million US dollars (MM USD)
MR	Mixed refrigerant
MRC	Mixed refrigerant cycle
NG	Natural gas
NGL	Natural gas liquid
Pbest	Particle best
PG	Propane gas
PS	Patter search
PSO	Particle swarm optimization
SMR	Single mixed refrigerant
TAC	Total annualized cost (MM USD)
TCC	Total capital cost (MM USD)
TEC	Total equipment cost (MM USD)
TOC	Total operating cost (MM USD)
UA	Overall heat transfer coefficient, U, multiplied by heat transfer area, A (kJ/sec-K)
Greek symbols	
α	Amortization factor
Symbols	
Ex	Exergy
h	Enthalpy
i	Interest rate (%)
m_{R1}^{DUAL}	Mass flow or stream R1 in dual nitrogen expansion process
$m_{MR,\ butane}^{SMR}$	Mass flow of stream MR's butane in SMR process
$m_{MR,ethane}^{SMR}$	Mass flow of stream MR's ethane in SMR process
$m_{MR,\ methane}^{SMR}$	Mass flow of stream MR's methane in SMR process
$m_{MR,\ nitrogen}^{SMR}$	Mass flow of stream MR's nitrogen in SMR process
$m_{MR,\ propane}^{SMR}$	Mass flow of stream MR's propane in SMR process
η_{ex}	Exergy efficiency (%)
n	Plant lifetime (year)
P_{R1}^{DUAL}	Pressure of stream LNG2 in dual nitrogen expansion process
P_{R2}^{DUAL}	Pressure of stream LNG2 in dual nitrogen expansion process

P^{SELF}_{NG2}	Pressure of stream NG2 in propane-precooling self-refrigeration process
P^{SELF}_{PG2}	Pressure of stream PG2 in propane-precooling self-refrigeration process
P^{SELF}_{PG4}	Pressure of stream PG4 in propane-precooling self-refrigeration process
P^{SMR}_{LNG2}	Pressure of stream LNG2 in SMR process
P^{SMR}_{MR2}	Pressure of stream MR2 in SMR process
s	Entropy
T^{DUAL}_{FEED}	Temperature of stream FEED in dual nitrogen expansion process
T^{DUAL}_{NG1}	Temperature of stream NG1 in dual nitrogen expansion process
T^{DUAL}_{NG2}	Temperature of stream NG2 in dual nitrogen expansion process
T^{DUAL}_{R3}	Temperature of stream R3 in dual nitrogen expansion process
T^{SELF}_{LNG1}	Temperature of stream LNG1 in propane-precooling self-refrigeration process
T^{SELF}_{NG4}	Temperature of stream NG4 in propane-precooling self-refrigeration process
$T^{SMR}_{LNG1,\ MR4}$	Temperature of stream LNG1 and MR4 in SMR process
$vf_{equipment}$	Vapor fraction of equipment
W	Net power consumed/produced (kW)
x^{DUAL}_{R9}	Split ratio of stream R9 in dual nitrogen expansion process

Appendix A

Appendix A.1. Schematics for Each Refrigerant Make up System

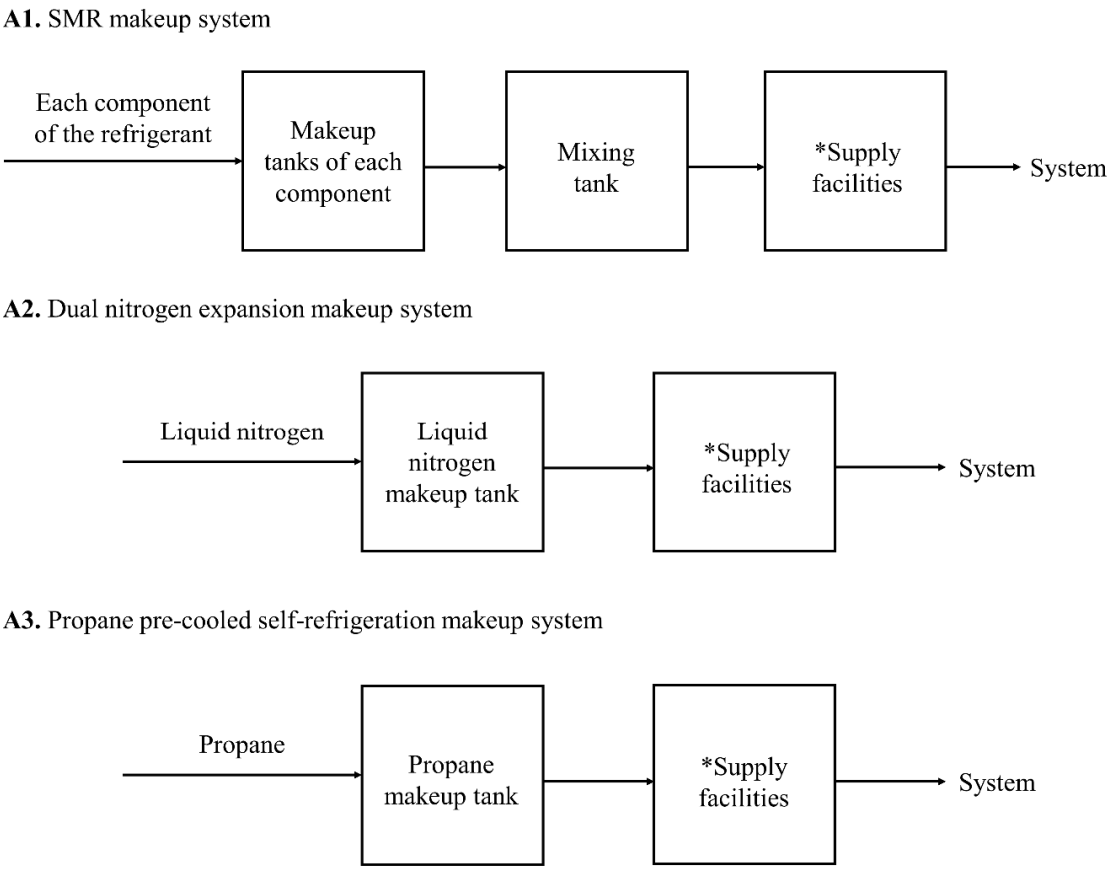

Figure A1. Refrigerant makeup systems for all processes; * The supply facilities consist of pumps and heaters.

Appendix A.2. Additional Constraints Values Used in the Sensitivity Analysis of Each Process

Table A1. Additional constraints for SMR.

Constraints	Value	Unit
UA of MCHE1	242.4	kJ/s-K
MR compressor duty	192.7	kW

Table A2. Additional constraints for dual nitrogen expansion.

Constraints	Value	Unit
UA of MCHE1	25.6	kJ/s-K
UA of MCHE2	22.7	
UA of MCHE2	5.5	kW
Warm expander duty	−100.1	
Cold expander duty	−14.8	
N_2 compressor duty	464.5	

Table A3. Additional constraints for propane pre-cooled self-refrigeration.

Constraints	Value	Unit
UA of MCHE1	7.3	kJ/s-K
UA of MCHE2	3.5	
Main compressor duty	154.4	kW
C_3 compressor duty	57.6	
Booster compressor duty	339.1	

Appendix A.3. Flowchart of PSO Algorithm

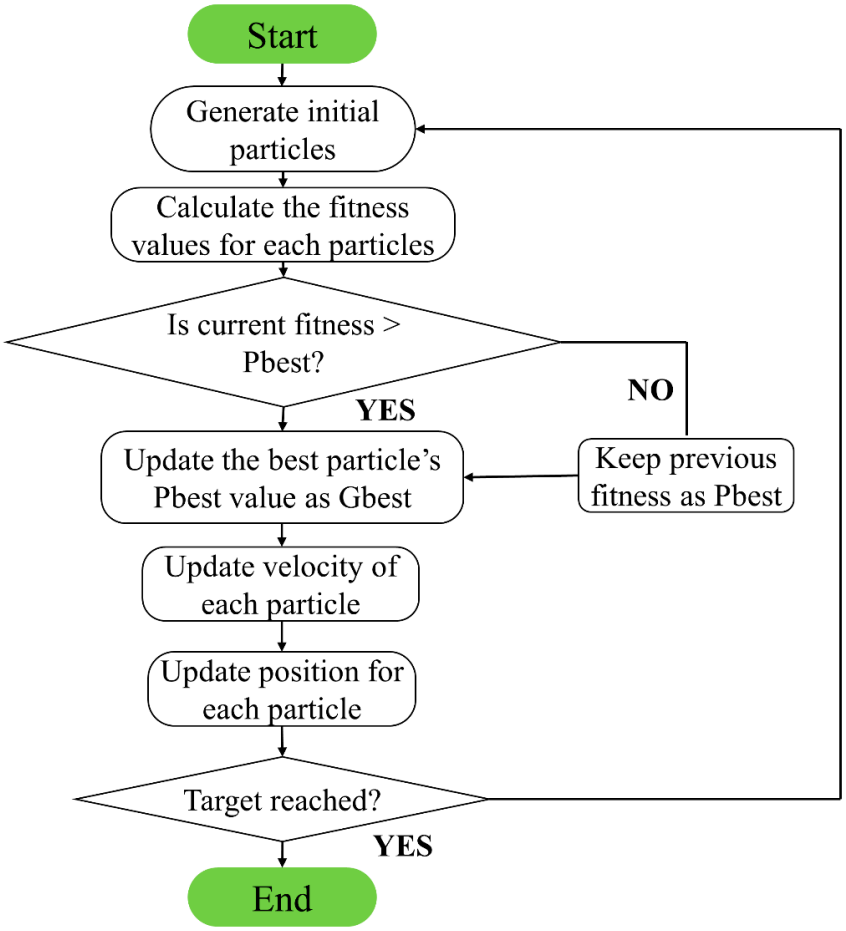

Figure A2. Flowchart of PSO algorithm.

Appendix A.4. Optimization Results of Each Process

This study conducted optimization to acquire the optimal value of the decision variables. The initial and optimized values for the decision variables of each process are summarized in Tables A1–A3.

Table A4. Optimization results for single mixed refrigerant.

Decision Variables	Initial Value	Optimized Value
Refrigerant mass flowrate (kg/h)		
Nitrogen	361.62	332.17
Methane	1056.19	456.65
Ethane	194.08	1303.89
Propane	512.32	0.01
N-Butane	1875.79	1936.80
JT-MR outlet pressure (bar)	2.5	3.76
Compressors discharge pressure (bar)	40	19.68
Hot stream outlet temperatures from MCHE (°C)	−148	−160.00
LNG production rate (tonne/year)		5346.6

Table A5. Optimization results for dual nitrogen expansion.

Decision Variables	Initial Value	Optimized Value
Refrigerant mass flowrate (kg/h)	7068	7361.56
N_2 compressors suction pressure (bar)	3	16.24
N_2 compressors discharge pressure (bar)	80	79.92
Warm/Cold expanders split ratio (R9)	0.42	0.75
Hot stream outlet temperatures from MCHE (°C)		
NG1	−22	−19.74
R4	−20	−25.29
NG2	−102	−101.95
R6	−95	−101.95
LNG1	−148	−158.68
LNG production rate (tonne/year)		5301.8

Table A6. Optimization results for propane pre-cooled self-refrigeration.

Decision Variables	Initial Value	Optimized Value
Propane mass flowrate (kg/h)	1100	1098.55
JT-PG outlet pressure (bar)	2	1.25
Main compressors discharge pressure (bar)	251.01	261.68
C_3 compressor discharge pressure (bar)	20.01	11.01
Hot stream outlet temperature from MCHE1 (°C)	−20	−35.33
Hot stream outlet temperature from MCHE2 (°C)	−69	−80.08
LNG production rate (tonne/year)		5487.3

References

1. Dudley, B. *BP Energy Outlook 2016*; BP: London, UK, 2016.
2. He, T.; Chong, Z.R.; Zheng, J.; Ju, Y.; Linga, P. LNG cold energy utilization: Prospects and challenges. *Energy* **2019**, *170*, 557–568. [CrossRef]
3. He, T.; Ju, Y. Optimal synthesis of expansion liquefaction cycle for distributed-scale LNG (liquefied natural gas) plant. *Energy* **2015**, *88*, 268–280. [CrossRef]
4. IGU. *IGU Releases 2017 World LNG Report*; IGU: Barcelona, Spain, 2017.
5. Ryu, J.; Lee, C.; Seo, Y.; Kim, J.; Seo, S.; Chang, D. A Novel Boil-Off Gas Re-Liquefaction Using a Spray Recondenser for Liquefied Natural-Gas Bunkering Operations. *Energies* **2016**, *9*, 1004. [CrossRef]
6. Price, B.; Mahaley, M.; Shimer, W. Optimize Small-Scale LNG Production with Modular SMR Technology. 2017. Available online: http://www.gasprocessingnews.com/features/201404/optimize-small-scale-lng-production-with-modular-smr-technology.aspx (accessed on 10 July 2020).
7. Seddon, D. *Gas Usage & Value*; PennWell: Tulsa, OK, USA, 2006; ISBN 1-59370-073-3.
8. Remeljej, C.; Hoadley, A. An exergy analysis of small-scale liquefied natural gas (LNG) liquefaction processes. *Energy* **2006**, *31*, 2005–2019. [CrossRef]
9. Khan, M.S.; Lee, M. Design optimization of single mixed refrigerant natural gas liquefaction process using the particle swarm paradigm with nonlinear constraints. *Energy* **2013**, *49*, 146–155. [CrossRef]
10. Qyyum, M.A.; He, T.; Qadeer, K.; Mao, N.; Lee, S.; Lee, M. Dual-effect single-mixed refrigeration cycle: An innovative alternative process for energy-efficient and cost-effective natural gas liquefaction. *Appl. Energy* **2020**, *268*, 115022. [CrossRef]
11. Qyyum, M.A.; Ali, W.; Long, N.V.D.; Khan, M.S.; Lee, M. Energy efficiency enhancement of a single mixed refrigerant LNG process using a novel hydraulic turbine. *Energy* **2018**, *144*, 968–976. [CrossRef]
12. He, T.; Mao, N.; Liu, Z.; Qyyum, M.A.; Lee, M.; Pravez, A.M. Impact of mixed refrigerant selection on energy and exergy performance of natural gas liquefaction processes. *Energy* **2020**, *199*, 117378. [CrossRef]
13. Qyyum, M.A.; Long, N.V.D.; Minh, L.Q.; Lee, M. Design optimization of single mixed refrigerant LNG process using a hybrid modified coordinate descent algorithm. *Cryogenics* **2018**, *89*, 131–140. [CrossRef]
14. Barclay, M.A. Thermodynamic Cycle Selection for Distributed Natural Gas Liquefaction. *AIP Conf. Proc.* **2004**, *710*, 75–82.

15. He, T.; Ju, Y. A novel conceptual design of parallel nitrogen expansion liquefaction process for small-scale LNG (liquefied natural gas) plant in skid-mount packages. *Energy* **2014**, *75*, 349–359. [CrossRef]
16. He, T.B.; Ju, Y.L. Performance improvement of nitrogen expansion liquefaction process for small-scale LNG plant. *Cryogenics* **2014**, *61*, 111–119. [CrossRef]
17. Yuan, Z.; Cui, M.; Xie, Y.; Li, C. Design and analysis of a small-scale natural gas liquefaction process adopting single nitrogen expansion with carbon dioxide pre-cooling. *Appl. Therm. Eng.* **2014**, *64*, 139–146. [CrossRef]
18. Abdul Qyyum, M.; Qadeer, K.; Lee, M. Closed-Loop Self-Cooling Recuperative N_2 Expander Cycle for the Energy Efficient and Ecological Natural Gas Liquefaction Process. *ACS Sustain. Chem. Eng.* **2018**, *6*, 5021–5033. [CrossRef]
19. Elbashir, N.O.; El-Halwagi, M.M.; Economou, I.G.; Hall, K.R. *Natural Gas Processing from Midstream to Downstream*; John Wiley & Sons: Hoboken, NJ, USA, 2018.
20. Breaking the Barriers of Small-Scale LNG: Galileo Launches the Cryobox. Available online: https://www.galileoar.com/en/galileo-launches-small-scale-lng-cryobox/ (accessed on 2 May 2020).
21. Ravikumar, A.P.; Roda-Stuart, D.; Liu, R.; Bradley, A.; Bergerson, J.; Nie, Y.; Zhang, S.; Bi, X.; Brandt, A.R. Repeated leak detection and repair surveys reduce methane emissions over scale of years. *Environ. Res. Lett.* **2020**, *15*, 034029. [CrossRef]
22. Kohler, T.; Bruentrup, M.; Engineering, L.; Key, R.D.; Edvardsson, T. Choose the best refrigeration technology for small-scale LNG production. *Hydrocarb. Process.* **2014**, *93*, 45–52.
23. Krishnamurthy, G.; Roberts, M.J.; Ott, C.M. Precooling strategies for efficient natural gas liquefaction. *Hydrocarb. Process.* **2017**, *96*, 19.
24. International Gas Union. Small Scale LNG. In Proceedings of the World Gas Conference (WGC Paris 2015), Paris, France, 1–5 June 2015.
25. Jeremi, M. *Distributed vs. Centralized Electricity Generation: Are We Witnessing A Change of Paradigm?* HEC Paris: Jouy-en-Josas, France, 2009.
26. Shirazi, L.; Sarmad, M.; Rostami, R.M.; Moein, P.; Zare, M.; Mohammadbeigy, K. Feasibility study of the small scale LNG plant infrastructure for gas supply in north of Iran (Case Study). *Sustain. Energy Technol. Assess.* **2019**, *35*, 220–229. [CrossRef]
27. Cao, L.; Liu, J.; Xu, X. Robustness analysis of the mixed refrigerant composition employed in the single mixed refrigerant (SMR) liquefied natural gas (LNG) process. *Appl. Therm. Eng.* **2016**, *93*, 1155–1163. [CrossRef]
28. Reverse Brayton Cycle—Brayton Refrigeration Cycle. Available online: https://www.nuclear-power.net/nuclear-engineering/thermodynamics/thermodynamic-cycles/heating-and-air-conditioning/reverse-brayton-cycle-brayton-refrigeration-cycle/ (accessed on 2 May 2020).
29. Gadhiraju, V. *Cryogenic Mixed Refrigerant Processes*; International Cryogenics Monograph Series; Timmerhaus, K.D., Rizzuto, C., Eds.; Springer: New York, NY, USA, 2008; ISBN 978-0-387-78513-4.
30. Bukowski, J.; Liu, Y.N.; Boccella, S.; Kowalski, L. *Innovations in Natural Gas Liquefaction Technology for Future LNG Plants and Floating Lng Facilities*; All from Air Products and Chemicals, Inc, International Has Union Research Conference; IGRC: Seoul, Korea, 2011.
31. Namdeo, R.; Manepatil, S.; Saraswat, S. *Detection of Valve Leakage in Reciprocating Compressor Using Artificial Neural Network (ANN)*; Purdue University: West Lafayette, IN, USA, 2008.
32. Compressed Air Leakage and Compressor Efficiency. Swagelok Indiana. Available online: https://indiana.swagelok.com/en/Tech-Resources/Blog---Tips-and-News/Compressed-Air-Leakage-and-Compressor-Efficiency (accessed on 1 June 2020).
33. Climate and Clean Air Coalition (CCAC). *Technical Guidance Document Number 4: Reciprocating Compressors Rod Seal/Packing Vents*; CCAC: Paris, France, 2017.
34. Ferreira, R.T.S.; Lilie, D.E.B. *Evaluation of the Leakage through the Clearance between Piston and Cylinder in Hermetic Compressors*; Purdue University: West Lafayette, IN, USA, 1984.
35. PARK, K.T. Transportable Refrigerant Supplying System for LNG Liquefaction Plant 2019. Patent Application Number 10-2017-0106470, 23 August 2017. [CrossRef]
36. Wang, B.; Huang, Y.; Wu, J.; Wang, T.; Lei, G. Experimental study on pressure control of liquid nitrogen tank by thermodynamic vent system. *Appl. Therm. Eng.* **2017**, *125*, 1037–1046. [CrossRef]
37. Wang, M.; Khalilpour, R.; Abbas, A. Thermodynamic and economic optimization of LNG mixed refrigerant processes. *Energy Convers. Manag.* **2014**, *88*, 947–961. [CrossRef]

38. He, T.; Liu, Z.; Ju, Y.; Parvez, A.M. A comprehensive optimization and comparison of modified single mixed refrigerant and parallel nitrogen expansion liquefaction process for small-scale mobile LNG plant. *Energy* **2019**, *167*, 1–12. [CrossRef]
39. Kim, J.; Seo, Y.; Chang, D. Economic evaluation of a new small-scale LNG supply chain using liquid nitrogen for natural-gas liquefaction. *Appl. Energy* **2016**, *182*, 154–163. [CrossRef]
40. Aspelund, A.; Gundersen, T.; Myklebust, J.; Nowak, M.P.; Tomasgard, A. An optimization-simulation model for a simple LNG process. *Comput. Chem. Eng.* **2010**, *34*, 1606–1617. [CrossRef]
41. Bao, J.; Lin, Y.; Zhang, R.; Zhang, N.; He, G. Effects of stage number of condensing process on the power generation systems for LNG cold energy recovery. *Appl. Therm. Eng.* **2017**, *126*, 566–582. [CrossRef]
42. Ansarinasab, H.; Mehrpooya, M.; Sadeghzadeh, M. An exergy-based investigation on hydrogen liquefaction plant-exergy, exergoeconomic, and exergoenvironmental analyses. *J. Clean. Prod.* **2019**, *210*, 530–541. [CrossRef]
43. Sadaghiani, M.S.; Mehrpooya, M.; Ansarinasab, H. Process development and exergy cost sensitivity analysis of a novel hydrogen liquefaction process. *Int. J. Hydrogen Energy* **2017**, *42*, 29797–29819. [CrossRef]
44. Park, K.; Oh, S.-R.; Won, W. Techno-economic optimization of the integration of an organic Rankine cycle into a molten carbonate fuel cell power plant. *Korean J. Chem. Eng.* **2019**, *36*, 345–355. [CrossRef]
45. Koo, J.; Oh, S.-R.; Choi, Y.-U.; Jung, J.-H.; Park, K. Optimization of an Organic Rankine Cycle System for an LNG-Powered Ship. *Energies* **2019**, *12*, 1933. [CrossRef]
46. Emadi, M.A.; Mahmoudimehr, J. Modeling and thermo-economic optimization of a new multi-generation system with geothermal heat source and LNG heat sink. *Energy Convers. Manag.* **2019**, *189*, 153–166. [CrossRef]
47. Akbari, N. Introducing and 3E (energy, exergy, economic) analysis of an integrated transcritical CO2 Rankine cycle, Stirling power cycle and LNG regasification process. *Appl. Therm. Eng.* **2018**, *140*, 442–454. [CrossRef]
48. Ghorbani, B.; Shirmohammadi, R.; Mehrpooya, M. A novel energy efficient LNG/NGL recovery process using absorption and mixed refrigerant refrigeration cycles—Economic and exergy analyses. *Appl. Therm. Eng.* **2018**, *132*, 283–295. [CrossRef]
49. Chong, Z.R.; He, T.; Babu, P.; Zheng, J.; Linga, P. Economic evaluation of energy efficient hydrate based desalination utilizing cold energy from liquefied natural gas (LNG). *Desalination* **2019**, *463*, 69–80. [CrossRef]
50. Rezaie, F.; Pirouzfar, V.; Alihosseini, A. Technical and economic analysis of acrylonitrile production from polypropylene. *Therm. Sci. Eng. Prog.* **2020**, *16*, 100463. [CrossRef]
51. Wang, T. U.S. average retail electricity prices 1990–2018 (in U.S. cents per kilowatt hour). *Stat. Res. Dep.* Available online: https://www.statista.com/statistics/711752/industrial-consumer-price-for-retail-electricity-in-mena-by-key-country/ (accessed on 12 April 2020).
52. Jenkins, S. 2019 CEPCI UPDATES: NOVEMBER (PRELIM.) AND OCTOBER (FINAL); Chemical Engineering Essentials for the CPI Professional. Available online: https://www.chemengonline.com/2019-cepci-updates-november-prelim-and-october-final (accessed on 27 January 2020).
53. Lozowki, D. The chemical engineering plant cost index; Chemical Engineering Essentials for the CPI Professional. Available online: https://www.chemengonline.com/pci-home/ (accessed on 27 January 2020).
54. Methane Prices, Liter. Available online: https://www.globalpetrolprices.com/methane_prices/ (accessed on 27 May 2020).
55. Ethane Prices. Available online: https://www.intratec.us/chemical-markets/ethane-price (accessed on 27 May 2020).
56. Propane Prices. Available online: https://www.intratec.us/chemical-markets/propane-price (accessed on 27 May 2020).
57. Butane Prices. Available online: https://www.intratec.us/chemical-markets/butane-price (accessed on 27 May 2020).
58. Sodium Prices. Available online: https://www.intratec.us/chemical-markets/sodium-price (accessed on 27 May 2020).
59. Songhurst, B. *LNG Plant Cost Escalation*; Oxford Institute for Energy Studies: Oxford, UK, 2014.

60. Graham, E.; Kenbar, A. LNG energy transfer uncertainty–sensitivity to composition and temperature changes. *Flow Meas. Instrum.* **2015**, *44*, 79–88. [CrossRef]
61. Schmid, D. Industrial sector electricity prices in the European Union (28 countries) between July and December 2017. *Stat. Res. Dep.* Available online: https://www.statista.com/statistics/263262/industrial-sector-electricity-prices-in-selected-european-countries/ (accessed on 5 June 2020).